Time-Resolved Absorption and Photothermal Measurements with Recombinant Sensory Rhodopsin II from *Natronobacterium pharaonis*

Aba Losi,* Ansgar A. Wegener,# Martin Engelhard,# Wolfgang Gärtner,* and Silvia E. Braslavsky*
*Max-Planck-Institut für Strahlenchemie, D-45413 Mülheim an der Ruhr, and #Max-Planck-Institut für Molekulare Physiologie, D-44139 Dortmund, Germany

ABSTRACT Purified wild-type sensory rhodopsin II from *Natronobacterium pharaonis* (pSRII-WT) and its histidine-tagged analog (pSRII-His) were studied by laser-induced optoacoustic spectroscopy (LIOAS) and flash photolysis with optical detection. The samples were either dissolved in detergent or reconstituted into polar lipids from purple membrane (PML). The quantum yield for the formation of the long-lived state M_{400} was determined as $\Phi_M = 0.5 \pm 0.06$ for both proteins. The structural volume change accompanying the production of K_{510} as determined with LIOAS was $\Delta V_{R,1} \leq 10$ ml for both proteins, assuming $\Phi_K \geq \Phi_M$, indicating that the His tag does not influence this early step of the photocycle. The medium has no influence on $\Delta V_{R,1}$, which is the largest so far measured for a retinal protein in this time range (<10 ns). This confirms the occurrence of conformational movements in pSRII for this step, as previously suggested by Fourier transform infrared spectroscopy. On the contrary, the decay of K_{510} is an expansion in the detergent-dissolved sample and a contraction in PML. Assuming an efficiency of 1.0, $\Delta V_{R,2} = -3$ ml/mol for pSRII-WT and -4.6 ml/mol for pSRII-His were calculated in PML, indicative of a small structural difference between the two proteins. The energy content of K_{510} is also affected by the tag. It is $E_K = (88 \pm 13)$ for pSRII-WT and (134 ± 11) kJ/mol for pSRII-His. A slight difference in the activation parameters for K_{510} decay confirms an influence of the C-terminal His on this step. At variance with $\Delta V_{R,1}$, the opposite sign of $\Delta V_{R,2}$ in detergent and PML suggests the occurrence of solvation effects on the decay of K_{510}, which are probably due to a different interaction of the active site with the two dissolving media.

INTRODUCTION

Photosensors that have a chromophore undergoing a *cis-trans* isomerization upon light absorption consist of retinal proteins such as the sensory rhodopsins in halobacteria (Hoff et al., 1997; Siebert, 1990; Spudich et al., 1995); open-chain tetrapyrrole-containing proteins, e.g., phytochromes in higher plants, in cyanobacteria, in some algae, and in ferns and mosses (Quail, 1997); and the xanthopsins, which contain the 4-hydroxycinnamoyl anion, such as the photoactive yellow protein (PYP) found in the eubacterium *Ectothiorhodospira halophila* (Kort et al., 1996; Rubinstenn et al., 1998; Meyer et al., 1987).

In all photoreceptors (certainly also in the photosensors) the nature of the chromophore-protein interaction is strongly linked to its particular function. Such interactions are responsible for the properties of these complex systems, which are in general fundamentally different from those of the separate chromophore and apoprotein entities. The fact that the same chromophore configuration linked to a slightly different apoprotein acts as an energy converter in bacteriorhodopsin (BR) and as a light sensor in sensory rhodopsins I and II underscores the specificity of those interactions (Oesterhelt, 1998).

In all photosensors with isomerizable chromophores, photoisomerization triggers a cascade of reactions involving conformational changes (in addition to the double-bond isomerization) in the chromophore and in the protein, the nature of which depends on the specific chromophore-protein interactions. Already upon formation of the early photoproducts, appearing in less than a few nanoseconds, the conformational changes result in structural volume changes (ΔV_R) that can be readily observed by means of temperature-dependent measurements with laser-induced optoacoustic spectroscopy (LIOAS) (Braslavsky and Heibel, 1992; Gensch et al., 1999; Schulenberg and Braslavsky, 1997).

In the photocycle of retinal proteins, retinal photoisomerization leads to the formation of an early red-shifted intermediate (called K in BR), on the subnanosecond time scale (Oesterhelt, 1998). By means of LIOAS it was possible to measure expansions associated with the production of the early intermediate, namely S_{610} in transducer-free sensory rhodopsin I (Losi et al., 1999) and bathorhodopsin in bovine rhodopsin (Rho) (Gensch et al., 1998), for which the ΔV_R values are +5.5 and +5 ml/mol, respectively. For the formation of K in BR, Zhang and Mauzerall (1996) reported an expansion of 1.5 ml/mol, whereas Schulenberg et al. (1994) observed a contraction of 11 ml/mol. The former appears to be a better value, for the reasons reported in the discussion.

The molecular origin of the structural volume changes accompanying the formation of the early intermediates in retinal proteins is still a matter of debate. Although the major conformational changes are expected to occur in the longer time ranges (ms to s) (Oesterhelt, 1998), data from

Received for publication 30 April 1999 and in final form 23 August 1999.
Address reprint requests to Dr. Silvia E. Braslavsky, Max-Planck-Institut für Strahlenchemie, Stiftstrasse 34-36, Postfach 10 13 65, D-45413 Mülheim an der Ruhr, Germany. Tel.: 49-208-306-3681; Fax: 49-208-306-3951; E-mail: braslavskys@mpi-muelheim.mpg.de.

0006-3495/99/12/3277/10 $2.00

low-temperature, Fourier transform infrared spectroscopy (FTIR) indicate that at the stage of the red-shifted intermediate, some conformational changes occur in the protein skeleton. These changes are very small in BR (Siebert and Mäntele, 1983) and are slightly more pronounced in Rho (Siebert, 1995). These conclusions cannot be directly extended to all sensory rhodopsins, inasmuch as S_{610} (the K-like intermediate) cannot be trapped at any temperature (Ariki et al., 1987) to obtain similar information for sensory rhodopsin I (SRI). On the contrary, sensory rhodopsin II from *Natronobacterium pharaonis* (pSRII, *pharaonis* sensory rhodopsin II) displays more favorable properties in view of the fact that FTIR data indicate that upon formation of K_{510} considerable conformational movements may take place (Engelhard et al., 1996). Furthermore, the photocycle of the protein is now well characterized (Chizov et al., 1998), and the stability of the photoreceptor toward low salt concentrations (Scharf et al., 1992) and high temperatures offers the possibility to vary the thermoelastic parameters of the solutions over a wide range, thus increasing the accuracy of the LIOAS measurements.

In this work we report the LIOAS determination of the structural volume changes and the energy level of the K_{510} intermediate in transducer-free pSRII, dissolved in detergent and reconstituted into polar purple membrane lipids (PMLs). Furthermore, we used flash photolysis for the estimation of the quantum yield for K_{510} production in the pSRII photocycle.

SRII is one of the four known retinylidene proteins in Archaebacteria (reviewed in Oesterhelt, 1998). It absorbs blue-green light in the energy peak of the solar spectrum and mediates a photophobic response; its chromophore is all-*trans* retinal (Imamoto et al., 1992) bound to a lysine residue through a protonated Schiff base. In vivo, SRII forms a complex with a transducer protein (HtrII, also an intrinsic membrane protein). The complex modulates a phosphotransfer cascade, eventually leading to the flagellar motor response (reviewed in Hoff et al., 1997). The purified, transducer-free pSRII absorbs with a maximum at 497 nm, and the photocycle proceeds through the following chromophore states (subscripts denote the maximum absorbance): K_{510}, L_{495}, M_{400}, N_{485}, and O_{535} (Chizov et al., 1998) named in analogy to the states in the photocycle of BR (reviewed in Lanyi and Varo, 1995). In sensory rhodopsins the presence of the transducer protein is known to alter the kinetics and the efficiency of the latest stages in the photocycle (Olson and Spudich, 1993; Sasaki and Spudich, 1998).

In M_{400} the chromophore is in a 13-*cis* conformation, and the Schiff base is deprotonated (Imamoto et al., 1992). The formation of M_{400} is probably accompanied by the protonation of Asp^{75} (Engelhard et al., 1996), as suggested by the fact that mutation of the corresponding Asp in the photoreceptor of *Halobacterium salinarum* (hSRII) into asparagine prevents the formation of M_{400} (Spudich et al., 1997).

The M_{400} species accumulates in the long microsecond time scale and decays to the parent state in ~500 ms, through a complex kinetic scheme (Chizov et al., 1998). Taking into account that the time window of LIOAS does not exceed the microsecond range, we now present data only for the early steps in the photoreceptor photocycle.

For the work reported here, pSRII was purified in a one-step procedure. The holoprotein was obtained after heterologous expression of photoactive protein in *Escherichia coli* (with an additional His-tagging at the C-terminus for purification purposes) and in the presence of all-*trans* retinal (Hohenfeld et al., 1999). To analyze the influence of these additional amino acids on the chromophore-protein interactions, the photochemical behavior of pSRII wild type (pSRII-WT) obtained upon expression in *Halobacterium salinarum* was compared with that of the His-tagged protein pSRII-His.

MATERIALS AND METHODS

Protein purification

The purification of pSRII-WT followed essentially the procedure described by Chizov et al. (1998), except that *n*-dodecyl-β-D-maltoside (DM) was used instead of *n*-octyl-β-D-glycoside. In the final chromatographic step the purified protein was concentrated on DEAE-Sepharose and eluted in low-DM buffer (0.025%) with 25 mM sodium phosphate (pH 8) and 500 mM NaCl, yielding a final pSRII-WT concentration of 4–5 mg/ml.

The overexpression and isolation of the pSRII-His fusion protein in *E. coli* was analogous to that described by Hohenfeld et al. (1999). The fraction eluting the Ni-NTA (nickel-nitrilo triacetic acid matrix; Qiagen, Hilden, Germany) column containing pSRII-His was adjusted to 70 mM NaCl and 25 mM sodium phosphate buffer (pH 8) (0.15% DM). Under these conditions pSRII-His does not bind on coupled CM-DEAE-columns. After NaCl removal, the pSRII-His solution was concentrated as described above.

The purity of the protein samples was judged by sodium dodecyl sulfate-polyacrylamide gel electrophoresis as well as by the ratio between the absorption at 280 nm and 500 nm. Our value of ≤ 1.3 indicates a purity of $\geq 95\%$.

Reconstitution into purple membrane polar lipids

PMLs were isolated according to the protocols of Kates (Kates et al., 1982). After fast injection of 1 ml lipid solution (50 mg/ml $CHCl_3$/MeOH, 65/35 v/v) into 50 ml 25 mM sodium phosphate (pH 8), the resulting suspension was homogenized in an ultrasonic bath and subsequently lyophilized to remove the organic solvents. Rehydration with an equal volume of water gives a slightly turbid and stable suspension.

For reconstitution, usually 1 ml of protein stock solution was mixed with the PML suspension to get a 1:20 or a 1:100 molar ratio. After gentle shaking for 30 min at room temperature the mixture was diluted by adding 4 volumes of 500 mM NaCl and 25 mM sodium phosphate (pH 8). DM was removed by incubating with a twofold excess of detergent adsorber gel (Boehringer-Mannheim) overnight at 7°C, following the methods of Rigaud et al. (1997) and Holloway (1973). The resulting membrane aggregates were filtered from the adsorber, sedimented at 80,000 × *g*, washed, and homogenized in 25 mM sodium phosphate buffer (pH 8), using a Branson Sonifier Microtip (20% output). The remaining aggregates were removed by sedimentation in a desktop centrifuge (8000 rpm) to reduce light scattering.

Chemicals

Bromocresol green and Evans blue, used as the calorimetric references, were from Sigma Chemical Co. (St. Louis, MO). 5,10,15,20-Tetrakis-(4-

sulfonatophenyl)-porphin (TSPP), used as an actinometric reference, was from Porphyrin Products (Logan, UT). DM was from Calbiochem-Novabiochem (La Jolla, CA).

Instrumentation

Absorption spectra were recorded with a Shimadzu UV-2102PC spectrophotometer.

Flash photolysis measurements were performed with the equipment already described by Ruddat et al. (1997). The sample concentration was around 5 μM, amounting to an absorbance of around 0.2 at 500 nm. Excitation at this wavelength was achieved by pumping the frequency-tripled pulse of a Nd:YAG laser (Spectron Laser System SL 456G, 6 ns pulse duration, 355 nm) into a Beta Barium Borate Optical Parametric Oscillator (OPO-C-355, bandwidth 420–515 nm; Laser Technik Vertriebs GmbH). The pulse was shaped to a circular spot of 2.5 cm diameter. A 100-W continuous-wave tungsten halogen lamp for detection in the millisecond-to-second range and a 150-W pulsed xenon arc for microsecond detection delivered the analyzing light. Transient absorption measurements were performed under magic angle conditions to avoid artifacts caused by rotational diffusion (Losi et al., 1999). A dual-beam detection arrangement compensated for fluctations in the analyzing beam intensity. Photomultiplier tubes (Hamamatsu R3896) served as detectors in the observation and reference pathways. The voltages were recorded with a transient digital oscilloscope (Tektronix TDS 520a) and transferred to a VAX station and a personal IBM computer for data analysis.

During the LIOAS experiments, excitation at 500 nm was achieved by means of a Lambda Physik-EMG101 MSC excimer laser (XeCl), pumping a FL2000 dye laser with Coumarin 307 dye (25-ns pulses, at 500 nm) or by employing the Nd:YAG/OPO system described above. Reference and sample absorbances were matched within 5% at the excitation wavelength. The beam was shaped by a slit (0.5 × 6 mm), which determines an acoustic transit time in aqueous solution of ~300 ns, allowing time resolution down to ~30 ns by the use of deconvolution techniques (Rudzki et al., 1985). The pulse fluence was varied with a neutral density filter and measured with a pyroelectric energy meter (RJP735 head connected to a RJ7620 meter from Laser Precision Corp.). The acoustic wave was detected by a Pb-Zr-Ti ceramic piezoelectric transducer (PZT) (4 mm; Vernitron), amplified 100 times (Comlinear E103), digitized by a digital oscilloscope (Tektronik TDS 684A, operating at 500 megasample/s), and stored in a VAX station 3100 and a personal computer for further treatment of the data. Normally, 100 signals were averaged for both the sample and the reference. Given the slow photocycle of the proteins, the pulse frequency was kept very low (around 0.3 Hz). Care was taken to perform the experiments in the linear regime of amplitude versus laser fluence, which was up to 30 μJ per pulse. The incident total energy per pulse actually employed was between 10 and 15 μJ per pulse, which corresponds to fluences between 330 and 500 μJ/cm^2.

The values of the ratio of thermoelastic parameters ($c_p\rho/\beta$) at the various temperatures were determined by comparing the LIOAS signal amplitude for the calorimetric reference in the buffer used and in neat water. In aqueous solutions the adiabatic compressibility is almost identical to the isothermal compressibility (Borsarelli and Braslavsky, 1997). Evans blue and bromocresol green were used as calorimetric reference compounds in neat water and in the buffer solutions, respectively. The concentration of DM was matched between the sample and reference preparations. For the PML-reconstituted proteins, the polar lipids (prepared as described above) where added to reference solutions to have the same scattering as in the sample preparations; possible small differences in the PML concentration (always in the μM range) between sample and reference are not supposed to alter the thermoelastic parameters of the buffer employed.

Treatment of LIOAS data

The time evolution of the pressure wave was assumed to be a sum of single-exponential functions. This function has proved to fit the decays of all other photoreceptors studied by LIOAS to date (Schulenberg and Braslavsky, 1997). The deconvolution analysis yielded the fractional amplitudes (φ_i) and the lifetimes (τ_i) of the transients (Sound Analysis 3000, Quantum Northwest, Spokane, WA). The time window was between 10 ns and 5 μs; decays faster than 10 ns were integrated by the piezoelectric transducer, while decays longer than 5 μs were not sensed.

The amplitudes (φ_i) recovered from deconvolution are related to the fluence-normalized heat released (q_i) and structural volume changes ($\Delta V_{r,i}$) by (Rudzki-Small et al., 1992; Rudzki et al., 1985)

$$\varphi_i = \frac{q_i}{E_\lambda} + \frac{\Delta V_{r,i}}{E_\lambda}\frac{c_p\rho}{\beta} \quad (1)$$

where E_λ is the molar excitation energy, $\beta = (\partial V/\partial T)_p\, 1/V$ is the volume expansion coefficient, c_p is the heat capacity at constant pressure, and ρ is the mass density of the solvent. Thus ($c_p\rho/\beta$) is the ratio of thermoelastic parameters of the solvent. $\Delta V_{r,i} = \Phi_i \Delta V_{R,i}$, where Φ_i is the quantum yield of the ith process and $\Delta V_{R,i}$ is the structural volume change per mole of phototransformed species. The variation in ($c_p\rho/\beta$) was achieved by varying the temperature, according to the several temperatures (ST) method, as previously described (van Brederode et al., 1995).

The fraction of absorbed energy released as heat in the ith step, $\alpha_{thi} = q_i/E_\lambda$, is then recovered from the intercept and $\Delta V_{r,i}$ from the slope of φ_i versus ($c_p\rho/\beta$) plots, provided that both parameters remain constant over the temperature range employed. Control measurements were also performed using the two temperatures (TT) method, where the sample is measured at the temperature for which $\beta = 0$ ($T_{\beta=0}$) and at a slightly higher temperature $T_{\beta>0}$, close enough to $T_{\beta=0}$ to assume the thermal compressibility to be unchanged. The reference solution was measured at the same $T_{\beta>0}$. α_{thi} and $\Delta V_{r,i}$ were calculated by taking into account the value of ($c_p\rho/\beta$) at this temperature (Malkin et al., 1994).

From simple energy balance considerations, "the prompt heat" release (α_{th1}) for all processes with lifetime $\tau_{pr} < 10$ ns is expressed by

$$\frac{q_1}{E_\lambda} = \alpha_{th1} = 1 - \Phi_K \frac{E_K}{E_\lambda} \quad (2)$$

where Φ_K and E_K are the quantum yield of formation of K_{510} and its energy level, respectively. Fluorescence can be neglected, because no emission was determined in the temperature range and in the solvents employed. Equation 2 implies that K_{510} is formed within 10 ns and decays on a longer time scale. The amplitude and lifetime associated with the decay of K_{510} (φ_2, τ_2) are recovered by means of the deconvolution algorithm described above, provided that τ_2 falls within the pressure integration window.

Therefore, given the known kinetics of the pSRII photocycle, we obtain the following information through the application of Eqs. 1 and 2: 1) α_{th1} and $\Delta V_{r,1}$, from which $\Delta V_{R,1}$ and E_K are derived, provided that Φ_K is known, and 2) α_{th2}, $\Delta V_{r,2}$, and τ_2 for the decay of K_{510}. The dependence of τ_2 on temperature should, furthermore, afford the activation parameters of K_{510} decay.

RESULTS

Quantum yield of the photocycle

The significant spectral overlap among the first intermediates of the pSRII photocycle (Chizov et al., 1998) strongly impairs the direct determination of Φ_K by optical methods. The bleaching of the parent state in the ms range, corresponding to the formation of M_{400}, is instead readily detected, and it remains for several ms. The determination of Φ_M is thus easier, but it may result in an underestimation of Φ_K, i.e., $\Phi_K \geq \Phi_M$, because a temperature-dependent equilibrium between M_{400} and L_{495} may occur (Chizov et al., 1998).

The comparative method in flash photolysis was applied (Bensasson et al., 1978), using TSPP as an actinometer, according to the procedure described by van Brederode et al. (1995). Fig. 1 shows the fluence (E_a) dependence of the triplet-triplet absorption of TSPP at 460 nm and the bleaching of the pSRII parent state in the ms region. Φ_M was calculated with

$$\Phi_M = \Phi_{TSPP}\frac{(\Delta A_{510}/E_a)_{pSRII}\varepsilon_{460,TSPP}}{(\Delta A_{460}/E_a)_{TSPP}\varepsilon_{510,pSRII}} \quad (3)$$

where $\Phi_{TSPP} = 0.6$ (Davila and Harriman, 1990), $\epsilon_{460,\ TSPP} = 47{,}000\ M^{-1}\ cm^{-1}$ (van Brederode et al., 1995); the value of $\epsilon_{510,\ pSRII} = 33000\ M^{-1}\ cm^{-1}$ was derived from the absorption spectrum of pSRII and $\epsilon_{498} = 40000\ M^{-1}\ cm^{-1}$ (Chizov et al., 1998). The results obtained from two sets of experiments in detergent solutions at room temperature were $\Phi_M = 0.51 \pm 0.06$ and $\Phi_M = 0.46 \pm 0.06$ for pSRII-WT and pSRII-His, respectively. No significant changes were observed with changes in the temperature between 5°C and 50°C, indicating that the possible thermal equilibrium between M_{400} and L_{495} either has a small influence on Φ_M or induces variations within the experimental error .

Comparative measurements between the PML reconstituted and the DM-dissolved proteins performed at the lowest and highest energies reported in Fig. 1 showed that there are no differences in Φ_M between the two preparations. This was also confirmed by the LIOAS experiments (see below).

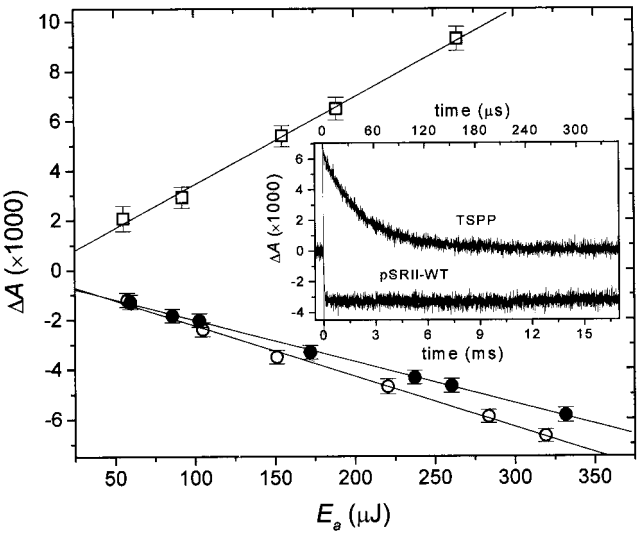

FIGURE 1 Determination of Φ_M by means of the comparative method in flash photolysis. Energy dependence of the amplitude of (□) the T-T absorption of TSPP monitored at 460 nm immediately after the laser pulse and of the bleaching of (○) detergent-dissolved pSRII-WT and (●]) pSRII-His, both monitored at 510 nm between 3 and 13 ms after the laser pulse. $T = 20$°C. $A_{500} = 0.2$, 25 mM sodium phosphate buffer, pH 8. The pSRII solutions also contained 0.025% DM, 50 mM NaCl for pSRII-WT and 10 mM NaCl for pSRII-His. *Inset*: Time evolution of the signals for TSPP and pSRII-WT.

LIOAS of pSRII: the formation and decay of K_{510}

Measurements were performed on four different sample preparations, as indicated in Table 1, i.e., detergent-solubilized samples at low (10 or 50 mM) and 150 mM NaCl concentration and proteins reconstituted in PML with 20:1 and 100:1 lipid-to-protein ratios. The PML preparations did not contain NaCl unless otherwise stated. All measurements were performed in 25 mM sodium phosphate buffer at pH 8. A typical room-temperature LIOAS signal is shown in Fig. 2, together with the fitting and residual functions recovered from the deconvolution procedure.

The occurrence of an expansion in the subnanosecond region is evident from the positive slope of the plots of φ_1 versus ($c_p\rho/\beta$) (Fig. 3). A deviation from linearity occurred in detergent at low NaCl concentration, at $T > 32$°C, for both pSRII-WT and pSRII-His. Inasmuch as no significant variation was detected in the absorption spectrum, this effect should be attributed to a temperature-induced mechanistic change above 32°C, i.e., a higher nonradiative conversion rate. Therefore, points at the highest temperature were excluded from the linear analysis (limited to detergent at low NaCl concentration).

Regarding the appearance of the first intermediate K_{510} the results were relatively similar for the two proteins (Table 1) as well as for the proteins in the various media employed, confirming the identity of quantum yields in the different preparations, as determined by flash photolysis. By applying the relationship $\Delta V_{r,i} = \Phi_i \Delta V_{R,i}$, a volume change of ~10 ml/mol is obtained for the process pSRII $\rightarrow K_{510}$. This value of $\Delta V_{R,1}$ must be considered as an upper limit, because $\Phi_M \leq \Phi_K$ (vide supra). The results obtained with the TT and ST methods are in general similar, and only the latter are reported in the LIOAS tables, unless otherwise indicated.

The value of α_{th1} is only slightly, but systematically, lower for pSRII-His. The difference between the two proteins is, on average, 7%, i.e., slightly larger than the experimental error (5%). The difference between the detergent and the PML preparations is, instead, ~4.5% for pSRII-WT and 0.5% for pSRII-His. This difference was therefore not taken as significant, and the energy content of K_{510} was calculated by averaging the value of α_{th1} for all preparations and separately for the two proteins. Taking into account the formation quantum yields $\Phi_M = 0.51 \pm 0.06$ (pSRII-WT) and $\Phi_M = 0.46 \pm 0.06$ (pSRII-His), and employing Eq. 2, we obtained for the energy content of K_{510} an average value of (88 ± 13) kJ/mol for pSRII-WT and (134 ± 11) kJ/mol for pSRII-His.

The φ_2 versus ($c_p\rho/\beta$) plots indicate a further expansion in the detergent-dissolved samples for the K_{510} decay. The linearity is, however, less sharp than for the subnanosecond step (see Fig. 4), and the errors derived from the average of two independent experiments (Table 2) are much larger.

For the PML samples (lipid-to-protein ratio 20:1), the situation changed drastically. A contraction characterized the K_{510} decay (Fig. 4). To rule out the possibility of protein

TABLE 1 LIOAS-derived parameters for the formation of K_{510} in potassium phosphate buffer, 25 mM, pH 8, λ_{exc} = 500 nm

	$\alpha_{th,1}$ ($\tau_1 < 10$ ns)	$\Delta V_{r,1}$ (ml/mol)	$\Delta V_{R,1}$ (ml/mol)	r*
pSRII-WT (DM, 50 mM NaCl)	0.82 ± 0.04	5.1 ± 1	10 ± 2	0.991
pSRII-WT (DM, 150 mM NaCl)	0.85 ± 0.05	4.9 ± 0.4	9.6 ± 0.8	0.991
pSRII-WT (PML, 20:1)	0.79 ± 0.05	4.8 ± 0.2	9.4 ± 0.4	0.993
pSRII-WT (PML, 100:1)	0.79 ± 0.04	4.4 ± 0.2	8.6 ± 0.4	0.993
pSRII-His (DM, 10 mM NaCl)	0.77 ± 0.04	4.7 ± 0.4	10.2 ± 0.9	0.998
pSRII-His (DM, 150 mM NaCl)	0.72 ± 0.04	4.6 ± 0.3	10 ± 0.6	0.990
pSRII-His (PML, 20:1)	0.73 ± 0.05	4.8 ± 0.2	10.2 ± 0.4	0.993
pSRII-His (PML, 100:1)	0.75 ± 0.04	4.3 ± 0.2	9.3 ± 0.4	0.994

The temperature range 6–54°C afforded a variation in ($c_p\rho/\beta$) between ~8 and ~70 kJ/mL. The concentration of DM was 0.025% in the low [NaCl] samples and 0.05% in the 150 mM NaCl preparations. For the PML samples the lipid-to-protein ratio is indicated.
*r, Variance of the linear regression with Eq. 1. Errors come from two sets of experiments in each case.

clusters inducing this effect, samples at a 100:1 lipid-to-protein ratio were also tested. The measurements afforded results similar to those of the 20:1 preparations (Table 2). The possible influence of NaCl was also ruled out because measurements of the PML preparations with 150 mM NaCl showed no difference with the samples devoid of salt (data not shown). For PML, the data obtained with the ST method were considerably different from those derived with the TT approach. The values of α_{th2} were too large ($\alpha_{th1} + \alpha_{th2} \geq 1$, in brackets in Table 2) in the former case. This may be related to the detection of the third decay (L → M) at the highest temperatures employed. A three-exponential analysis, however, did not improve the results. The problems are probably mainly due to a large scattering of these preparations and to the bad resolution of LIOAS in the μs region, given that the subsequent decay, $L_{495} \rightarrow M_{400}$, should have a lifetime of some μs at the highest temperatures employed (37–52°C) (Chizov et al., 1998). For the PML preparations the TT method affords $\alpha_{th1} + \alpha_{th2} \approx 1$ (Table 2).

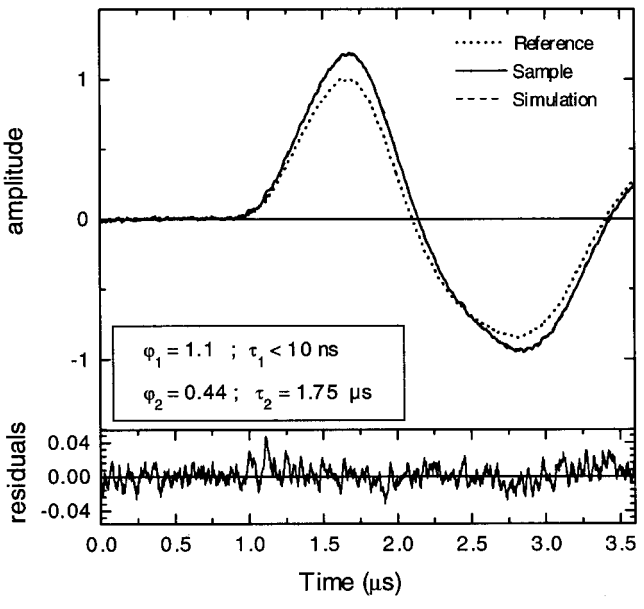

FIGURE 2 LIOAS waveform of (——) DM-dissolved pSRII-His and of (·····) bromocresol green, recorded at 20°C. The reconvoluted curve is nearly perfectly superimposed on the sample waveform. The residual distribution and the results of deconvolution are also shown. Note that the sample signal is larger than the reference, because of the positive $\Delta V_{r,1}$ contribution.

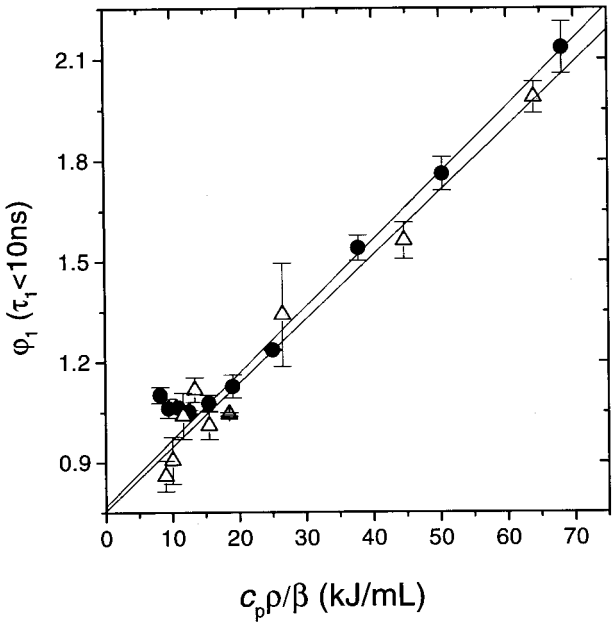

FIGURE 3 Amplitude of the fast component (φ_1) with lifetime $\tau_1 < 10$ ns, after deconvolution of LIOAS waveforms, versus ($c_p\rho/\beta$) for (●) DM-dissolved pSRII-His (10 mM NaCl) and (△) pSRII-His reconstituted in PML at a lipid-to-protein ratio of 20:1. Note the deviation from linearity at the highest temperatures (lowest values of $c_p\rho/\beta$) for the DM preparation. The error bars arise from the deconvolution of four waveforms at each temperature.

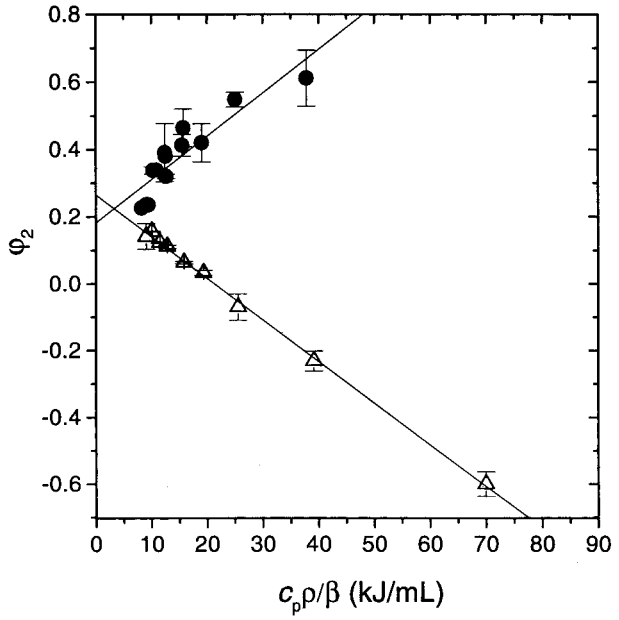

FIGURE 4 Amplitudes φ_2 of the slower component with lifetime 10 ns $< \tau_2 <$ 5 μs, detected by deconvolution of LIOAS waveforms versus ($c_p\rho/\beta$), corresponding to the decay of K_{510}. ●, DM-dissolved pSRII-His (10 mM NaCl); △, pSRII-His in PML, lipid-to-protein ratio 20:1. The error bars arise from the deconvolution of four waveforms at each temperature.

The activation parameters derived from the linear fitting of the plots of $\ln(1/\tau_2)$ versus $1/T$ (Table 3 and Fig. 5) are similar for the detergent-dissolved samples at 150 mM NaCl concentration and for the PML preparations. The activation energy E_a is around 40 kJ/mol, while the preexponential factor A is between 1 and 9 $\times$ 10^{12} s^{-1}. This supports the concept that, despite the opposite sign of $\Delta V_{r,2}$, this decay corresponds to the same step in the photocycle, namely the decay $K_{510} \rightarrow L_{495}$. Transient absorption experiments have in fact provided evidence that the intermediates formed in DM and in PML are spectroscopically and kinetically similar. Only for the proteins in DM at low salt concentration both activation parameters seem to decrease.

TABLE 2 LIOAS-derived parameters for the decay of K_{510}, as recovered by the deconvolution procedure

	α_{th2}	$\Delta V_{r,2}$ (ml/mol)	r*
pSRII-WT (DM, 50 mM NaCl)	0.09 ± 0.04	5.6 ± 0.7	0.908
pSRII-WT (DM, 150 mM NaCl)	0.02 ± 0.02	8.8 ± 0.5	0.994
pSRII-WT	0.2 ± 0.05	−2 ± 0.6	
(PML, 20:1)	(0.38 ± 0.15)	(−5.5 ± 2)	(0.865)
pSRII-WT	0.25 ± 0.05	−1 ± 0.3	
(PML, 100:1)	(0.39 ± 0.04)	(−1.7 ± 0.3)	(0.991)
pSRII-His (DM, 10 mM NaCl)	0.10 ± 0.04	3.1 ± 0.5	0.903
pSRII-His (DM, 150 mM NaCl)	0.04 ± 0.04	6.4 ± 2.2	0.891
pSRII-His	0.18 ± 0.05	−2.8 ± 0.7	
(PML, 20:1)	(0.27 ± 0.05)	(−3 ± 0.2)	(0.986)
pSRII-His	0.25 ± 0.05	−1.5 ± 0.7	
(PML, 100:1)	(0.37 ± 0.05)	(−2.3 ± 0.2)	(0.981)

Conditions are as in Table 1. For the PML preparations the results from the ST method are reported in brackets. For the TT experiments, $T_{\beta=0}$ = 3.5°C for PML 20:1 and 3.2°C for PML. $T_{\beta>0}$ = 7°C.
*r, Variance of the linear regression with Eq. 1. Errors come from two sets of experiments in each case.

TABLE 3 Activation energy (E_a) and preexponential factor (A) for the decay of K_{510}, from the linear fitting of the $\ln(1/\tau_2)$ versus $1/T$ plots

	A (s^{-1}) $\times$ 10^{-12}	E_a (kJ/mol)	r*
pSRII-WT (DM, 50 mM NaCl)	0.2	31 ± 1	0.998
pSRII-WT (DM, 150 mM NaCl)	9	40 ± 2	0.995
pSRII-WT (PML, 20:1)	8.1	40 ± 2	0.981
pSRII-His (DM, 10 mM NaCl)	0.022	26 ± 1	0.995
pSRII-His (DM, 150 mM NaCl)	7.3	40 ± 5	0.991
pSRII-His (PML, 20:1)	1.2	35 ± 2	0.982

τ_2 is the lifetime associated with the φ_2 amplitudes in LIOAS deconvolution.
*r, Variance of the linear regression. Errors come from two sets of experiments in each case.

DISCUSSION

The available quantum yields and LIOAS parameters related to the early step in the photocycle of retinal proteins

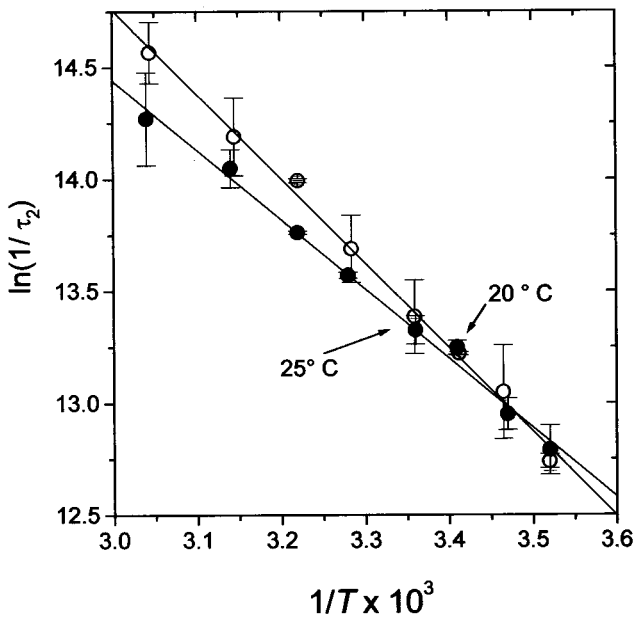

FIGURE 5 Arrhenius plot $\ln(1/\tau_2)$ versus $1/T$ for pSRII-WT and pSRII-His, detergent-dissolved, at 50 mM and 10 mM NaCl, respectively. τ_2 is as derived from the deconvolution of LIOAS waveforms. Straight lines are the linear fittings according to the Arrhenius equation (see Table 3 for results); T range = 11–56°C; τ_2 range = 3 μs to 470 ns for pSRII-WT and 3 μs to 640 ns for pSRII-His. Experimental conditions are as in Table 1.

are collected in Table 4, where Φ_{PI} (photoisomerization quantum yield) is the quantum yield of formation of the early red-shifted intermediate. So far sensory rhodopsins have been studied by LIOAS only as transducer-free proteins, and no LIOAS data have been reported for halorhodopsin.

Quantum yields

The values of Φ_{PI} ranges between 0.4 (SRI) (Losi et al., 1999) and 0.67 (rhodopsin) (Dartnall, 1972). The direct determination of $\Phi_{PI} = \Phi_K$ by means of the comparative method in flash photolysis is in general difficult because of the spectral overlapping of this transient with the parent state. The method employed in this paper for pSRII, namely the bleaching of the parent state in an appropriate time region, has already been successfully applied to BR (Tittor and Oesterhelt, 1990) and rhodopsin (Dartnall, 1972), but it implies that all the steps after the photoisomerization occur with unit efficiency. This was not the case for transducer-free SRI, for which the formation of S_{610} was employed as a parameter (Losi et al., 1999) and may lead to an underestimation of Φ_K in the case of pSRII (Chizov et al., 1998). In any case, the similarity of the quantum yields as reported above (Fig. 1) indicates that the His tag does not interfere with the efficiency of the photoisomerization step.

Volume changes

For all of the retinal proteins so far investigated by means of LIOAS, the formation of the red-shifted intermediate is accompanied by a structural volume change. For BR two different values, +1.5 and −11 ml/mol, have been reported by Zhang and Mauzerall (1996) and by Schulenberg et al. (1994), respectively. In the latter case, a relatively high photon fluence and the need for a high concentration of the calorimetric reference are most probably the reasons for an erroneous result. Since then we have utilized as calorimetric references organic dyes with larger absorption coefficients in the visible than the inorganic salts (Losi et al., 1999). However, other effects complicate the measurements with BR, such as the possible existence of more than one transient in the ns to μs time range (unpublished data).

The ΔV_R associated with the K-like appearance ranges, therefore, from a very small expansion in BR, corresponding to 2.5 Å^3 per molecule, to a much larger value in pSRII (corresponding to 16.5 Å^3 per molecule). This is likely to be related to local rearrangements of the amino acid residues in the retinal pocket. Electrostrictive effects are not thought to contribute extensively because there is no charge release during these steps and the variation in the dipole moment of the bare chromophore upon isomerization was calculated to be very small (Locknar and Peteanu, 1998). Interestingly, FTIR spectroscopy of K_{510} from pSRII trapped at low temperature has shown strong bands in the amide I region (Engelhard et al., 1996). This is in contrast to the case of BR, for which the corresponding amide I changes in K are much smaller (Siebert and Mäntele, 1983). The results reported here confirm that these spectral changes are indeed related to conformational movements in the protein skeleton, already at the stage of K_{510}.

The relative constant value of $\Delta V_{R,1}$ for pSRII upon changes in the microenvironment strongly supports the idea that it reflects an intrinsic conformational change, with little involvement of solvation effects. Smaller values of $\Delta V_{R,1}$ in the other retinal proteins may thus reflect smaller conformational movements at this level. The identity between the $\Delta V_{R,1}$ values for pSRII-WT and the pSRII-His indicates again (as in the case of the Φ_M values) that the histidine tag, added for purification purposes, does not interfere with the production of K_{510}.

The sign and magnitude of $\Delta V_{R,1}$ should be correlated with the entropy changes accompanying this step. The positive sign of $\Delta V_{R,1}$ for all retinal proteins, including rhodopsin, qualitatively indicates that $\Delta S_{R,1} > 0$, regardless of the direction of retinal isomerization. This implies that the formation of the red-shifted intermediate induces a weakening of the interactions between the chromophore and the adjacent molecules (i.e., hydrogen bonds with water or adjacent lateral groups of amino acids) and/or protein movements that result in a protein conformation that is more flexible than the parent state. For the calculation of $\Delta S_{R,K}$ with $\Delta V_{R,1}$ we cannot assume as valid the Maxwell equation ($\Delta S_R = \beta/\kappa_T$) that regards the solvent as a continuum (Morais and Zimmt, 1995). Taking into account that the retinal cavity is polar and hydrogen or ionic bonds are

TABLE 4 Retinal proteins: Φ_{PI}, ΔV_R, and energy levels (E_I) of the early, red-shifted intermediate in retinal proteins

	Φ_{PI}	ΔV_R (ml/mol)	E_I^* (kJ/mol)	E_I/E_{00} (%)	
SRI → S_{610}[#]	0.40	+5.5	142	76	Losi et al. (1999)
pSRII-WT → K_{510}[#§]	0.50	+10	88	40	This work
pSRII-His → K_{510}[#§]	0.46	+10	134	60	This work
BR → K[¶]	0.65	+1.5	55	28	Zhang and Mauzerall (1996)
Rho → Batho[‖]	0.67	+5	207	93	Gensch et al. (1998)

*Obtained upon dividing the reported total stored energy (36 kJ/mol) by Φ_{PI}.
[#]DM dissolved.
[§]PML reconstituted.
[¶]Purple membrane fragments.
[‖]Washed membranes.

established between the chromophore and adjacent residues, we tentatively employed the relationship proved to be valid in aqueous solutions for electron transfer reactions, $T\Delta S_{R,i} = X\Delta V_{R,i}$, where $X = 13$ kJ/ml (Borsarelli and Braslavsky, 1999). In these systems the change in the order of the medium (strongly hydrogen bound to the dissolved chromophore) determined the relationship $T\Delta S_{R,i} = X\Delta V_{R,i}$. With this relationship and $\Delta V_{R,1} = 10$ ml/mol for pSRII, the entropic term for the production of K_{510} is $T\,\Delta S_{R,K} = 130$ kJ/mol and $\Delta S_{R,K} = 440$ J/(mol K) at room temperature.

Energy storage

In retinal proteins, the fraction of energy released as heat upon formation of the early red-shifted (K-like) intermediate is quite large (Table 4). Upon subtracting the vibrational relaxation from the excited Frank-Condon state to $E_{0\text{-}0}$ (derived from the crossing of the normalized absorption and fluorescence spectra), the fraction of energy released promptly from $E_{0\text{-}0}$ as the respective first intermediate is produced, amounts to 60% in SRI and to 70% in pSRII and BR from the respective excitation wavelength (excitation at 580, 500, and 532 nm, respectively, corresponding to 206, 240, and 225 kJ/mol). The energy jump from the $E_{0\text{-}0}$ level to K-like intermediates (fourth column in Table 4) seems to be linearly correlated with Φ_{PI}; i.e., this step seems to be largely enthalpically driven. This correlation holds only for these strictly related systems, containing the same chromophore and undergoing similar photophysics.

The $E_{0\text{-}0}$ value for pSRII is not known. We have assumed that it lies between 10 and 20 kJ/mol below the energy of the transition corresponding to the absorption maximum, in analogy to the other retinal proteins (Losi et al., 1999; Guzzo and Pool, 1968; Birge and Zhang, 1990). $E_{0\text{-}0}$ should thus be between 220 and 230 kJ/mol. Taking the values for the energy content of the K_{510} intermediate as $E_K = (88 \pm 13)$ kJ/mol for pSRII-WT and $E_K = (134 \pm 11)$ kJ/mol for pSRII-His, energy steps are calculated to be ~40% and ~60%, respectively. We note that the errors of the energy levels are quite large, making the difference between the two values relatively small.

With the entropic term $T\Delta S_{R,K}$ calculated above, and bearing in mind that strong assumptions have been made regarding the validity of this calculation, values of $\Delta G_{R,K} \approx -40$ kJ/mol and $\Delta G_{R,K} \approx 0$ are calculated for the formation of K_{510} from ground-state pSRII-WT and pSRII-His, respectively. Clearly, for pSRII-WT, the entropy change more than compensates for the enthalpy change in K_{510} with respect to the parent state. This means that, provided our calculation of $T\Delta S_{R,K}$ is valid, K_{510} formation from the pSRII-WT ground state is thermodynamically spontaneous but kinetically controlled by the high activation barrier of the isomerization.

On the other hand, the back thermal process $K_{510} \rightarrow$ pSRII-WT, in addition to being kinetically impaired by an activation barrier, is thermodynamically uphill, with a $\Delta G_{K\rightarrow pSRII} = 40$ kJ/mol, and mainly entropically controlled, which forces the system to the next intermediates. The situation is slightly changed for pSRII-His, because of the higher energy content of K_{510}. $\Delta G_{R,K}$ for this modified protein makes the back-reaction $K_{510} \rightarrow$ pSRII-His thermodynamically more favorable.

The validity of our calculations clearly depends on the validity of the entropy estimation from ΔV_R. Notwithstanding this assessment, the larger volume changes measured for sensory rhodopsin I and, especially, for pSRII, are at least qualitatively consistent with a larger entropy change in this step, with respect to BR. This is most probably related to the greater rigidity of the retinal cavity in the sensory rhodopsins in the ground state, as indicated by the selective binding of all-*trans* retinal in these proteins, with no thermal equilibrium between the 13-*cis* and all-*trans* forms in the dark (Hoff et al., 1997). The retinal photoisomerization may thus induce a larger perturbation of the retinal cavity, with disruption of a larger number of weak interactions and/or larger modifications in the protein skeleton.

The decay of K_{510}

The second amplitude (φ_2) and the lifetime (τ_2) recovered by deconvolution in the ns to μs time scale should be associated with the decay of K_{510} into L_{495}. The lifetimes at room temperature correspond to those previously reported (around 1 μs) from flash photolysis (Chizov et al., 1998). The activation parameters, however, are very different. In particular, Chizov et al. reported values of $\Delta H^{\#} = 74$ kJ/mol and $\Delta S^{\#} = 120$ J mol^{-1}K^{-1} for pSRII-WT reconstituted in membranes (with a lipid-to-protein ratio similar to our 20:1 preparations). This corresponds to $E_a \approx 72$ kJ/mol and $A \approx 1 \times 10^{19}$ s^{-1}, at variance with the present results (Table 3). The discrepancy may be due to the different time resolutions of the two techniques. LIOAS is highly sensitive in the hundreds of ns to the short μs time region, whereas in the work of Chizov et al. (1998) the low time resolution in the short μs region did not allow clear discrimination of this time constant at $T > 35$°C. Furthermore, the absorption changes associated with the $K_{510} \rightarrow L_{495}$ decay are very small in flash photolysis, because of the strong spectral overlap between the two species. Although in principle LIOAS should give more reliable kinetic results for these reasons, the ST method, which extends to higher temperatures, also gives wrong results because of the overlapping longer lifetimes at those higher temperatures.

The opposite sign of $\Delta V_{r,2}$ for detergent-dissolved and PML samples (Table 2) could be accounted for by a strong influence of the dissolving medium during the decay $K_{510} \rightarrow L_{495}$. The former sign is similar to the case of the detergent-dissolved mutant D76N-SRI ($\Delta V_{r,2} \approx 2$ ml/mol), while the latter is similar to the contraction accompanying the $K_{510} \rightarrow L_{495}$ decay in membrane-embedded BR (Zhang and Mauzerall, 1996) ($\Delta V_{R,2} = -2.2$ ml/mol).

Assuming unitary efficiency, in the PML preparations average values of $\Delta V_{R,2} = -3$ ml/mol and -4.6 ml/mol for

pSRII-WT and pSRII-His, respectively, are calculated for K_{510} decay, i.e., a slightly larger contraction than in BR. For BR the contraction was attributed to the rearrangement of water in the protein matrix (Zhang and Mauzerall, 1996), and it was not observed for detergent-dissolved BR. The structural differences between pSRII and K_{510} are not known in such detail as to allow similar conclusions, and the contraction observed is in any case larger than that for BR. Taking into account that the total structural volume change is the sum of an intrinsic and a solvent-determined volume change, a different accessibility of the active site to the solvent in pSRII-WT and in pSRII-His could induce major differences in the solvent-determined portion of the volume change and thus account for the difference in sign in the total measured structural volume change. The intrinsic volume change is expected to be a contraction because in the L state stronger hydrogen bonds and salt bridges are expected (at least in BR; Oesterhelt, 1998), whereas medium effects are expected to result in expansions in L, precisely because stronger intrinsic interaction might weaken the interactions with the solvent.

Accordingly, the pK_a of the Schiff base counterion Asp^{75} was determined as 3.5 in DM and 5.6 in PML, suggesting that the interaction of pSRII with the detergent exposes other ionizable groups, in turn influencing the pK_a of the counterion complex (Chizov et al., 1998). In the mutated protein pSRII-D75N, the pK_a of the Schiff base is also influenced in a complex way by the dissolving medium (DM versus PML), indicating that the Schiff base itself or residues influencing its pK_a are surrounded by a different microenvironment in the two media (Losi et al., manuscript in preparation).

At variance with the lack of effect on the appearance of K_{510}, the histidine tag affects its decay. The values of (88 $\pm$ 13) kJ/mol for pSRII-WT and (134 $\pm$ 11) kJ/mol for pSRII-His, representing a storage of 37 and 56%, respectively, of the excitation energy, show that the energy stored in K_{510} is also somewhat different for the two proteins.

CONCLUSIONS

The photoisomerization of retinal in pSRII, which results in the formation of K_{510}, induces protein movements that are restricted to the active site and thus are almost insensitive to the solubilizing medium. This is a strong indication of the inaccessibility of the retinal cavity to the solvent at this early stage in the photocycle. The changes should involve amino acid residues close to the retinal pocket as well as modifications of hydrogen bonds and steric interactions between the Schiff base and the adjacent residues. On the contrary, the movements accompanying the decay of K_{510} are markedly influenced by the dissolving medium and are slightly sensitive to the introduction of the C-terminal His-tag. This suggests that at this stage the active site is more exposed to the solvent and that the conformational movements involve more peripheral portions of the protein skeleton.

The able technical assistance of Gudrun Klihm and Dagmar Lenk is greatly appreciated. We are indebted to Prof. Kurt Schaffner for his continuous generous support.

AL was supported by Marie Curie grant ERBFMBICT972377.

REFERENCES

Ariki, M., Y. Schichida, and T. Yoshizawa. 1987. Low temperature spectrophotometry on the photoreaction cycle of sensory rhodopsin. *FEBS Lett.* 225:255–258.

Bensasson, R., C. R. Goldschmidt, E. J. Land, and T. G. Truscott. 1978. Laser intensity and the comparative method for determination of triplet quantum yields. *Photochem. Photobiol.* 28:277–281.

Birge, R. R., and C.-F. Zhang. 1990. Two-photon double resonance spectroscopy of bacteriorhodopsin. Assignment of the electronic and dipolar properties of the low-lying 1A*g–like and 1B*u+-like Π, Π* states. *J. Chem. Phys.* 92:7178–7195.

Borsarelli, C. D., and S. E. Braslavsky. 1997. Nature of the water structure inside the pools of reversed micelles sensed by laser-induced optoacoustic spectroscopy. *J. Phys. Chem. B.* 101:6036–6042.

Borsarelli, C. D., and S. E. Braslavsky. 1999. Enthalpy, volume and entropy changes associated with the electron transfer reaction between the ^{3}MLCT state of $Ru(bpy)_3^{2+}$ and methylviologen cation in aqueous solutions. *J. Phys. Chem. A.* 103:1719–1727.

Braslavsky, S. E., and G. E. Heibel. 1992. Time-resolved photothermal and photoacoustic methods applied to photoinduced processes in solution. *Chem. Rev.* 92:1381–1410.

Chizov, I., G. Schmies, R. Seidel, J. R. Sydor, B. Lüttenberg, and M. Engelhard. 1998. The photophobic receptor from *Natronobacterium pharaonis*: temperature and pH dependencies of the photocycle of sensory rhodopsin II. *Biophys. J.* 75:999–1009.

Dartnall, H. J. A. 1972. Handbook of Sensory Physiology VII/1. Photochemistry of Vision. Photosensivity. Springer Verlag, New York.

Davila, J., and A. Harriman. 1990. Photoreactions of macrocyclic dyes bound to human serum albumin. *Photochem. Photobiol.* 51:9–19.

Engelhard, M., B. Scharf, and F. Siebert. 1996. Protonation changes during the photocycle of sensory rhodopsin II from *Natronobacterium pharaonis. FEBS Lett.* 395:195–198.

Gensch, T., J. M. Strassburger, W. Gärtner, and S. E. Braslavsky. 1998. Volume and enthalpy changes upon photoexcitation of bovine rhodopsin derived from optoacoustic studies by using an equilibrium between bathorhodopsin and blue-shifted intermediate. *Isr. J. Chem.* 38:231–236.

Gensch, T., C. Viappiani, and S. E. Braslavsky. 1999. Laser-induced time-resolved optoacoustic spectroscopy in solution. *In* Encyclopedia of Spectroscopy and Spectrometry: Photoacoustic Spectrometers. J. C. Lindon, G. E. Tranter, and J. L. Holmes, editors. Academic Press, London (in press).

Guzzo, A. V., and G. L. Pool. 1968. Visual pigment fluorescence. *Science.* 159:312–314.

Hoff, W. D., K.-H. Jung, and J. L. Spudich. 1997. Molecular mechanism of photosignaling by archaeal sensory rhodopsins. *Annu. Rev. Biophys. Biomol. Struct.* 26:223–258.

Hohenfeld, I. P., A. A. Wegener, and M. Engelhard. 1999. Purification of histidine tagged bacteriorhodopsin, *pharaonis* halorhodopsin and *pharaonis* sensory rhodopsin II functionally expressed in *Escherichia coli. FEBS Lett.* 442:198–202.

Holloway, P. M. 1973. Simple procedure for removal of Triton X-100 from protein samples. *Anal. Biochem.* 53:304–308.

Imamoto, Y., Y. Shichida, J. Hirayama, H. Tomioka, N. Kamo, and T. Yoshizawa. 1992. Chromophore configuration of *pharaonis* phoborhodopsin and its isomerization on photon absorption. *Biochemistry.* 31: 2523–2528.

Kates, M., S. C. Kushwaha, and G. D. Sprott. 1982. Lipids of purple membrane from extreme halophiles and of methanogenic bacteria. *Methods Enzymol.* 88:98–111.

Kort, R., H. Vonk, X. Xu, W. D. Hoff, W. Crielaard, and K. J. Hellingwerf. 1996. Evidence for *trans-cis* isomerization of the *p*-coumaric acid chromophore as the photochemical basis of the photocycle of photoactive yellow protein. *FEBS Lett.* 382:73–78.

Lanyi, J. K., and G. Varo. 1995. The photocycles of bacteriorhodopsin. *Isr. J. Chem.* 35:365–385.

Locknar, S. A., and L. A. Peteanu. 1998. Investigation of the relationship between dipolar properties and *cis-trans* configuration in retinal polyenes: a comparative study using Stark spectroscopy and semiempirical calculations. *J. Phys. Chem. B.* 102:4240–4246.

Losi, A., S. E. Braslavsky, W. Gärtner, and J. Spudich. 1999. Time-resolved absorption and photothermal measurements with sensory rhodopsin I from *Halobacterium salinarum. Biophys. J.* 76:2183–2191.

Malkin, S., M. S. Churio, S. Shochat, and S. E. Braslavsky. 1994. Photochemical energy storage and volume changes in the microsecond time range in bacterial photosynthesis—a laser induced optoacoustic study. *J. Photochem. Photobiol. B Biol.* 23:79–85.

Meyer, T. E., E. Yakali, M. A. Cusanovich, and G. Tollin. 1987. Properties of a water-soluble, yellow protein isolated from a halophilic phototrophic bacterium that has photochemical activity analogous to sensory rhodopsin. *Biochemistry.* 26:418–423.

Morais, J., and M. B. Zimmt. 1995. Thermodynamics of intramolecular electron transfer in alkane solvents. *J. Phys. Chem.* 99:8863–8871.

Oesterhelt, D. 1998. The structure and mechanism of the family of retinal proteins from halophilic bacteria. *Curr. Opin. Struct. Biol.* 8:489–500.

Olson, K. D., and J. L. Spudich. 1993. Removal of the transducer protein from sensory rhodopsin I exposes sites of proton release and uptake during the receptor photocycle. *Biophys. J.* 65:2578–2585.

Quail, P. 1997. The phytochromes: a biochemical mechanism of signaling in sight? *BioEssays.* 19:571–579.

Rigaud, J. L., G. Mosser, J. J. Lacapere, A. Olofsson, D. Levy, and J. L. Ranck. 1997. Bio-beads: an efficient strategy for two-dimensional crystallization of membrane proteins. *J. Struct. Biol.* 118:226–235.

Rubinstenn, G., G. W. Vuister, F. A. A. Mulder, P. E. Dux, R. Boelens, K. J. Hellingwerf, and R. Kaptein. 1998. Structural and dynamic changes of photoactive yellow protein during its photocycle in solution. *Nature Struct. Biol.* 5:568–570.

Ruddat, A., P. Schmidt, C. Gatz, S. E. Braslavsky, W. Gärtner, and K. Schaffner. 1997. Recombinant type A and B phytochromes from potato. Transient absorption spectroscopy. *Biochemistry.* 36:103–111.

Rudzki, J. E., J. L. Goodman, and K. S. Peters. 1985. Simultaneous determination of photoreaction dynamics and energetics using pulsed, time-resolved photoacoustic calorimetry. *J. Am. Chem. Soc.* 107: 7849–7854.

Rudzki-Small, J., L. J. Libertini, and E. W. Small. 1992. Analysis of photoacoustic waveforms using the nonlinear least square method. *Biophys. Chem.* 41:29–48.

Sasaki, J., and J. Spudich. 1998. The transducer protein HtrII modulates the lifetimes of sensory rhodopsin II photointermediates. *Biophys. J.* 75: 2435–2440.

Scharf, B., B. Pevec, B. Hess, and M. Engelhard. 1992. Biochemical and photochemical properties of the photophobic receptors from *Halobacterium halobium* and *Natronobacterium pharaonis. Eur. J. Biochem.* 206:359–366.

Schulenberg, P., and S. E. Braslavsky. 1997. Time-resolved photothermal studies with biological supramolecular systems. *In* Progress in Photothermal and Photoacoustic Science and Technology, Vol. 3, Life and Earth Sciences. A. Mandelis and P. Hess, editors. SPIE, Bellingham, WA. 58–81.

Schulenberg, P., M. Rohr, W. Gärtner, and S. E. Braslavsky. 1994. Photoinduced volume changes associated with the early transformations of bacteriorhodopsin: a laser-induced optoacoustic spectroscopy study. *Biophys. J.* 66:838–843.

Siebert, F. 1990. Retinal proteins. *In* Photochromism: Molecules and Systems. H. Dürr and H. Bouas-Laurent, editors. Elsevier, Amsterdam. 756–792.

Siebert, F. 1995. Application of FTIR spectroscopy to the investigation of dark structures and photoreactions of visual pigments. *Isr. J. Chem.* 35:309–323.

Siebert, F., and W. Mäntele. 1983. Investigation of the primary photochemistry of bacteriorhodopsin by low-temperature Fourier transform infrared spectroscopy. *Eur. J. Biochem.* 130:565–573.

Spudich, J. L., D. N. Zacks, and R. A. Bogomolni. 1995. Microbial sensory rhodopsin: photochemistry and function. *Isr. J. Chem.* 35:495–513.

Spudich, E. N., W. S. Zhang, M. Alam, and J. L. Spudich. 1997. Constitutive signaling by the phototaxis receptor sensory rhodopsin II from disruption of its protonated Schiff base Asp-73 interhelical salt bridge. *Proc. Natl. Acad. Sci. USA.* 94:4960–4965.

Tittor, J., and D. Oesterhelt. 1990. The quantum yield of bacteriorhodopsin. *FEBS Lett.* 263:269–273

van Brederode, M. E., T. Gensch, W. D. Hoff, K. J. Hellingwerf, and S. E. Braslavsky. 1995. Photoinduced volume change and energy storage associated with the early transformations of the photoactive yellow protein from *Ectothiorhodospira halophila. Biophys. J.* 68:1101–1109.

Zhang, H., and D. Mauzerall. 1996. Volume and enthalpy changes in the early steps of bacteriorhodopsin photocycle studied by time-resolved photoacoustics. *Biophys. J.* 71:381–388.